Degradation of Methylene Blue by Heterogeneous Fenton Reaction Using Titanomagnetite at Neutral pH Values: Process and Affecting Factors

Shijian Yang,[†,‡] Hongping He,*[,†] Daqing Wu,[†] Dong Chen,[§] Yuehong Ma,[†,‡] Xiaoli Li,[||] Jianxi Zhu,[†] and Peng Yuan[†]

Guangzhou Institute of Geochemistry, Chinese Academy of Sciences, Guangzhou 510640, PR China, Graduate School of the Chinese Academy of Sciences, Beijing 100039, PR China, School of Resources & Environmental Engineering, Hefei University of Technology, Hefei 230009, PR China, and Environmental Monitoring Central Station of Suqian City, Suqian 223800, PR China

In this work, titanomagnetite was used as a heterogeneous Fenton catalyst for the degradation of methylene blue (MB). The degradation of MB on synthetic titanomagnetite at neutral pH values was studied in comparison with the adsorption of MB on titanomagnetite using UV−vis, FTIR, and the analyses of element C on titanomagnetite and DOC in reaction solution. Meanwhile, important factors affecting catalytic activity were investigated, that is, titanomagnetite load, H_2O_2 concentration, and reaction temperature. Titanomagnetite decomposed H_2O_2 yielding highly reactive hydroxyl radicals, and MB adsorbed on titanomagnetite was degraded. With the increases of titanomagnetite load, H_2O_2 concentration, and reaction temperature, the degradation of MB was promoted. Moreover, titanomagnetite was proved to be durable with a stable MB removal efficiency after five consecutive cycles.

1. Introduction

A powerful method for the remediation of wastewater is chemical oxidation. Hydroxyl radical ($^{\bullet}OH$) is often chosen because it is a nonspecific oxidant which can react with most organic contaminants at near diffusion-limited rates.[1−3] The common way to make hydroxyl radicals is to inject acidified solution of ferrous ions into the wastewater, followed by concentrated H_2O_2. This is the well-known Fenton reaction:[4,5]

$$Fe^{2+} + H_2O_2 \rightarrow Fe^{3+} + {}^{\bullet}OH + OH^- \quad (1)$$

But there are some disadvantages for the application of the homogeneous Fenton process, including the requirement of low pH, the formation of a significant amount of ferric hydroxide sludge in the course of Fenton treatment, and the requirements of further separation and disposal for the resulting sludge.[6,7]

So heterogeneous Fenton reaction for the degradation of organic contaminants has been described, in which iron oxides or Fe hydroxides are often employed.[8,9] Unfortunately, the requirement of UV light for photocatalysis, unsuitable pH-dependence of activity, strong ferric ion leaching due to low pH, and the difficulty of catalyst recovery limit the use of the process.[8−12]

Recent studies demonstrate that magnetite is the most effective catalyst as compared with other iron oxides,[3,13,14] possibly because it is the only one that has Fe^{2+} in its structure to enhance the production rate of $^{\bullet}OH$.[3] Meanwhile, its inherent magnetism makes it easy to be separated from the reaction system. More recently, it is reported that the introduction of Co, Cr, and Mn into magnetite structure to form $Fe_{3-x}Co_xO_4$, $Fe_{3-x}Cr_xO_4$, and $Fe_{3-x}Mn_xO_4$ can strongly promote the degradation of methylene blue (MB) due to a significant promotion of H_2O_2 decomposition.[15−20]

In our previous work, it was demonstrated that the introduction of Ti into magnetite structure to form $Fe_{3-x}Ti_xO_4$ can also promote the decolorization of MB. But the promotion may be mainly attributed to the significant increase of MB adsorbed on $Fe_{3-x}Ti_xO_4$.[21] In this paper, we try to describe the process of MB degradation on titanomagnetite in comparison with the adsorption of MB on titanomagnetite. Furthermore, some important factors affecting catalytic activity will be investigated.

2. Experimental Procedure

2.1. Preparation of Titanomagnetite. Powdered titanomagnetite and magnetite were prepared as outlined in our previous work.[21] In titanomagnetite, the ratio of Ti to Fe was about 1:3. The characterization of X-ray diffraction and Mössbauer spectroscopy shows that both synthetic magnetite and titanomagnetite were spinel structures, Ti was introduced into the structure of titanomagnetite, and the average diameters of synthetic titanomagnetite and magnetite particles were both about 120 nm (the details are shown in Supporting Information).[21]

2.2. Characterization. Surface areas were determined by the BET method using N_2 adsorption−desorption isotherms. N_2 adsorption−desorption isotherms were measured on a gas sorption analyzer (Quantachrome, NOVA 1000) at a liquid nitrogen temperature. Prior to measurement, samples were outgassed at 150 °C and a pressure less than 10^{-3} Torr for 6 h. The particle size and morphology were examined using scanning electronic microscopy (SEM). The vacuum-dried samples were used for SEM analysis, which was carried out on a FEI QUSNTA-400 electron microscope. Fourier transform infrared spectra (FTIR) were recorded on a Vector 33 Fourier transform infrared spectrometer. Sixty-four scans were collected for each measurement in the spectral range of 400−4000 cm^{-1} with a resolution of 4 cm^{-1}. Specimens for FTIR measurement were prepared as follows: 5 mg of the sample powder was mixed with 95 mg of KBr. Subsequently, the mixture was pressed into a pellet.

* To whom correspondence should be addressed. Tel.: +86-20-85290257. Fax: +86-20-85290130. E-mail: hehp@gig.ac.cn.
[†] Guangzhou Institute of Geochemistry, Chinese Academy of Sciences.
[‡] Graduate School of the Chinese Academy of Sciences.
[§] Hefei University of Technology.
[||] Environmental Monitoring Central Station of Suqian City.

10.1021/ie900666b CCC: $40.75
Published on Web 09/10/2009

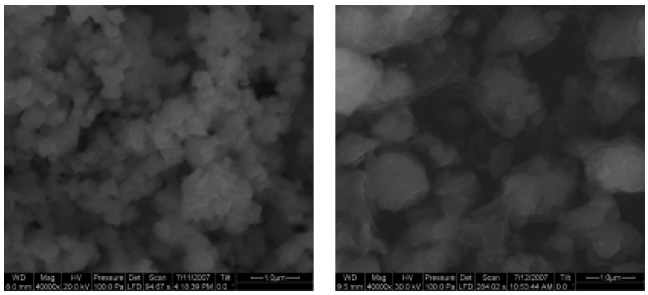

a b

Figure 1. SEM images of (a) synthetic magnetite and (b) synthetic titanomagnetite.

2.3. Reaction Systems. The degradation of MB on synthetic titanomagnetite at pH 6.8 and room temperature (about 30 °C) were carried out in a glass reactor (containing 400 mL of reaction solution) equipped with a magnetic stirrer. The reaction was started by the addition of MB or H_2O_2. If not specific mentioned, titanomagnetite load and initial concentrations of H_2O_2 and MB were 1.0 g L^{-1}, 0.30 mol L^{-1}, and 100 mg L^{-1}, respectively. During the reaction, the system was continuously stirred at 500 rpm, and little titanomagnetite adhered to the stirrer. At each sampling time, 5 mL of the suspension was sampled from the reactor. Immediately, titanomagnetite was separated by centrifugation at 3500 rpm for 3 min. Then, 2.00 mL of the supernatant was sampled and diluted for UV−vis spectra and dissolved organic carbon (DOC) analyses. The separated titanomagnetite was collected and dried in a vacuum oven at 100 °C for 24 h for element C, N and FTIR analyses. It was decided not to stop the reaction by the addition of a quenching agent because this interfered with the analysis of the reaction mixture.[22] In the experiments with the pH-dependence, the pH values were adjusted to pH 6.8 using a buffer solution (KH_2PO_4 + NaOH). It was proved by FTIR spectra that little phosphate adsorbed on titanomagnetite at pH 6.8. The degree of MB removed from reaction solution was expressed as the percent decrease of absorbance at absorption maximum of 665 nm. DOC concentration in reaction solution was determined using a Shimadzu TOC-V_{CPH} analyzer, and element C and N contents on dry titanomagnetite were examined using a Vario EL III element analyzer. The amount of aniline compounds in reaction solution after the treatment was determined spectrophotometrically with *N*-(1-naphthyl)-ethylenediamine.

3. Results and Discussion

3.1. Characterization of Synthetic Titanomagnetite. To observe synthetic magnetite and titanomagnetite, SEM was employed, and the images are shown in Figure 1. The images show regular octahedrons with very smooth surfaces, which indicates that the particles were well crystallized. As shown in Figure 1a, the particles in synthetic magnetite arranged compactly because of the conglomeration. But some particles in synthetic titanomagnetite were separated (shown in Figure 1b). It may result from the reduction of magnetization due to the introduction of Ti into magnetite structure.[23] So the BET surface area of synthetic titanomagnetite was 20.7 m^2 g^{-1}, which was much more than the BET surface area of synthetic magnetite (6.65 m^2 g^{-1}).

3.2. Degradation of MB on Titanomagnetite. Catalytic Activity of Synthetic Titanomagnetite. Removal of MB by synthetic magnetite and titanomagnetite (3.0 g L^{-1}) in the presence of H_2O_2 at pH 6.8 was conducted (shown in Figure 2). It shows that, as compared with magnetite, the removal of

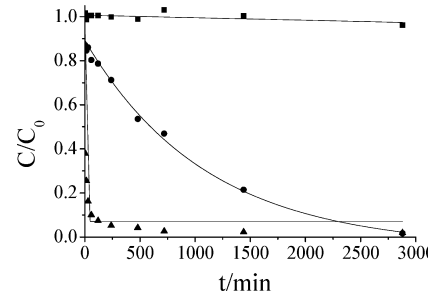

Figure 2. Removal of MB by magnetite and titanomagnetite (3.0 g L^{-1}) in the presence of H_2O_2: ■, blank experiment (MB + H_2O_2); ●, magnetite; ▲, titanomagnetite.

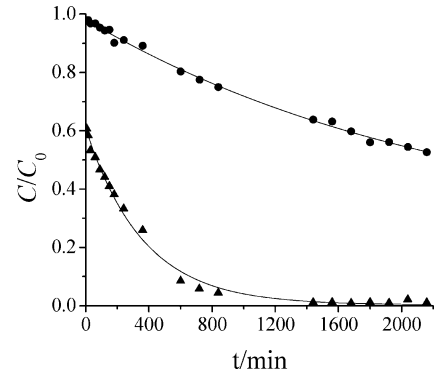

Figure 3. Degradation of MB on magnetite and titanomagnetite, in which H_2O_2 was added after the addition of MB for 12 h: ●, magnetite; ▲, titanomagnetite.

MB by titanomagnetite in the presence of H_2O_2 was promoted remarkably. In this instance, the removal of MB from reaction solution resulted from both adsorption and degradation. To describe the degradation of MB on magnetite and titanomagnetite clearly, another experiment was conducted. In the experiment, H_2O_2 was added after the addition of MB for 12 h. The degradation of organics on iron oxides in the presence of H_2O_2 may be attributed to the radical mechanism.[2,10,24−27] In previous research, MB was used as a test for rapid qualitative detection of hydroxyl radical.[28] As shown in Figure 2, no MB was removed in the blank experiment. It indicates that no hydroxyl radical formed without magnetite or titanomagnetite. As shown in Figure 3, although the adsorption of MB on magnetite and titanomagnetite had reached adsorption equilibrium at time zero, MB in the reaction solution was further removed after the addition of H_2O_2. It demonstrates that hydroxyl radical was generated from the catalytic decomposition of H_2O_2 by titanomagnetite or magnetite. So in Figure 3, the further removal of MB after the addition of H_2O_2 (time zero) should be attributed to the degradation of MB on synthetic titanomagnetite (or magnetite).

The degradation of MB was fitted to the following pseudo-first-order kinetics:

$$-\mathrm{d}C/\mathrm{d}t = kC \tag{2}$$

$$\ln(C/C_0') = -kt \tag{3}$$

where C and C_0' are the concentrations of MB in reaction solution at time t and zero, respectively; t is the reaction time, and k is the pseudo-first-order kinetic constant.

The pseudo-first-order kinetic constants k for the degradation of MB on magnetite and titanomagnetite (Figure 3) are displayed

Table 1. Pseudo-first-order Kinetic Constant (k) and Correlation Coefficient (R^2) for the Degradation of MB

Catalyst	H_2O_2 concentration (mol L^{-1})	Temperature (°C)	K (min^{-1})	R^2
magnetite	0.30	room temperature	4.30×10^{-4}	0.997
titanomagnetite	0.075	room temperature	1.10×10^{-3}	0.991
titanomagnetite	0.15	room temperature	1.43×10^{-3}	0.994
titanomagnetite	0.30	room temperature	2.15×10^{-3}	0.994
titanomagnetite	0.45	room temperature	3.14×10^{-3}	0.995
titanomagnetite	0.30	35	2.35×10^{-3}	0.996
titanomagnetite	0.30	50	8.52×10^{-3}	0.999
titanomagnetite	0.30	70	3.47×10^{-2}	0.997

in Table 1. It implies that titanomagnetite shows a more excellent catalytic activity than magnetite for the degradation of MB.

UV−Vis Spectra Study. The temporal evolutions of UV−vis spectra taking place during the removal of MB by titanomagnetite (3.0 g L^{-1}) are displayed in Figure 4. In the absence of H_2O_2, the absorbances at 247, 292, 620, and 665 nm which are characteristic absorptions of MB decreased gradually, and no other peaks appeared (shown in Figure 4a). This indicates that, in the absence of H_2O_2, no MB was degraded and the removal of MB from reaction solution was attributed to the adsorption of MB on titanomagnetite. Because of the intense absorption of H_2O_2 at about 200 nm (proved by the experiment using pure H_2O_2), some slight changes in UV−vis spectra are difficult to observe (shown in Figure 4b,c). To show the changes in UV−vis spectra clearly, the spectral lines corresponding to 5 min were used as baselines and subtracted from all spectral lines. After this treatment, Figure 4b,c was transformed into Figure 4d,e, respectively. In Figure 4d,e, the positive peaks correspond to the appearance of the degradation products and the negative peaks correspond to the decrease of MB or H_2O_2.[21] In Figure 4d, the negative peak at 200 nm corresponds to the decomposition of H_2O_2, and the peaks at 247, 292, 620, and 665 nm correspond to the removal of MB. Meanwhile, some positive peaks at 220, 265, and 310 nm can be observed in Figure 4d. The occurrence of the peak at 220 nm implies the formation of NO_3^-,[29−31] and the peak at 265 nm may be ascribed to another degradation product. In Figure 4e, the peak at 310 nm did not appear. So the appearance of this peak in Figure 4d is attributed to the superposition of the positive peak at 265 nm and the negative peak at 292 nm. According to the appearance of the degradation products, it can be concluded that some MB was degraded by titanomagnetite in the presence of H_2O_2.

Mineralization of MB. To verify the mineralization during the degradation of MB on titanomagnetite, DOC concentration in reaction solution and element C content on dry titanomagnetite were both determined. DOC concentration reflects the total amount of organics in reaction solution, and element C content presents the total amount of organics adsorbed on titanomagnetite. During the adsorption of MB on titanomagnetite, DOC and MB concentrations in reaction solution decreased and element C content on titanomagnetite increased (shown in Figure 5a). Changes of DOC concentration in reaction solution and element C content on dry titanomagnetite during the degradation of MB on titanomagnetite are displayed in Figure 5b,c. As shown in Figure 5b, at the first 30 min, DOC concentration in reaction solution decreased and element C content on titanomagnetite increased during the removal of MB. This is mainly attributed to the adsorption of MB on titanomagnetite. Subsequently, element C content on titanomagnetite

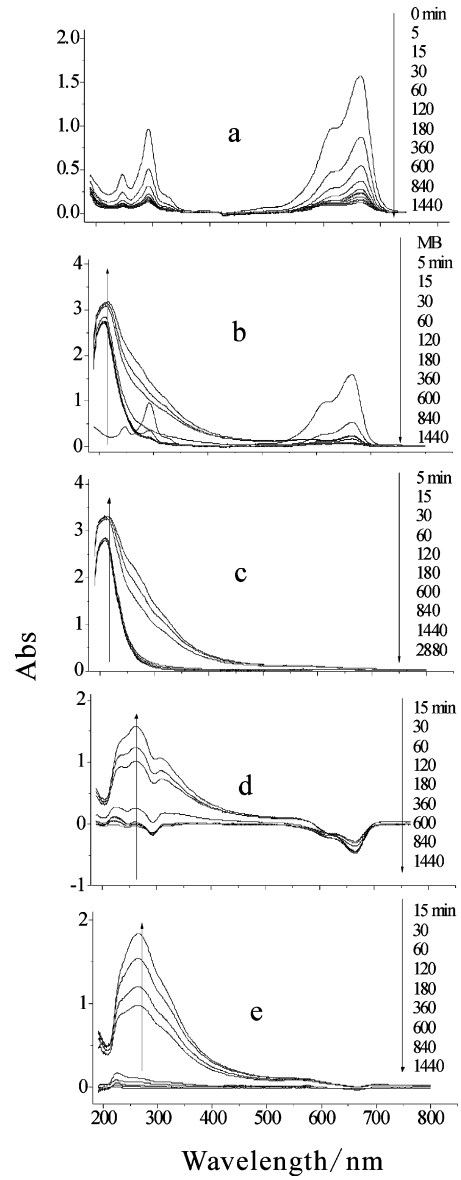

Figure 4. Changes of UV−vis spectra during the removal of MB by titanomagnetite: (a) no H_2O_2 was added; (b) MB and H_2O_2 were added synchronously; (c) after the addition of MB for 12 h, H_2O_2 was added; (d) transformation of b; and (e) transformation of c.

decreased and DOC concentration in reaction solution increased with the degradation of MB on titanomagnetite. It may be largely attributed to the weak affinity of titanomagnetite for the organic degradation products at neutral pH values.[21] As a result, the degradation products desorbed from titanomagnetite and entered reaction solution. This is further proved in Figure 5c. At time zero, there was little MB in the reaction solution, and most MB was adsorbed on titanomagnetite. So element C content on titanomagnetite was at the maximum. After the addition of H_2O_2, MB adsorbed on titanomagnetite was degraded gradually. Meanwhile, the degradation products desorbed from titanomagnetite due to the weak affinity of titanomagnetite for them at neutral pH values. As a result, element C content on titanomagnetite decreased and DOC concentration in reaction solution increased. Taking account of DOC in the reaction solution and element C on titanomagnetite, little MB was mineralized during the degradation of MB on titanomagnetite at neutral pH values.

As shown in Figure 5b, there were little MB in the reaction solution and a small amount of element C on titanomagnetite

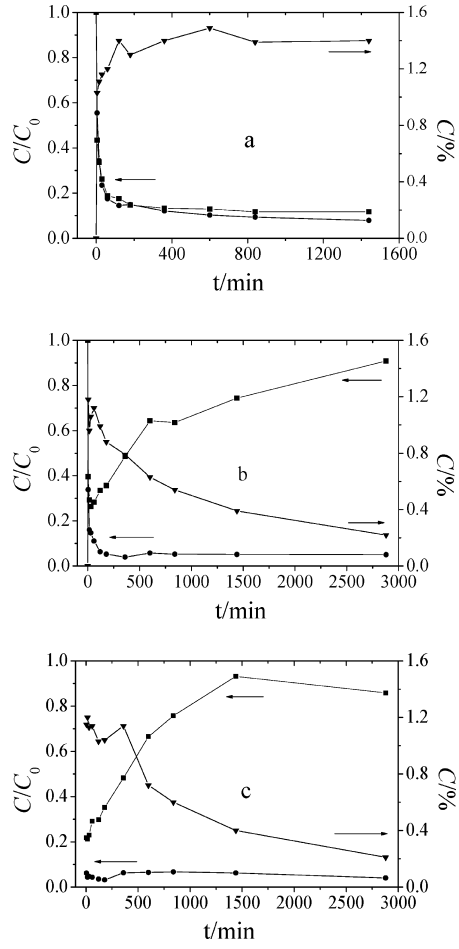

Figure 5. Changes of DOC, MB concentrations in reaction solution, and element C content on titanomagnetite during the removal of MB by titanomagnetite: (a) no H_2O_2 was added; (b) MB and H_2O_2 were added synchronously; (c) after the addition of MB for 12 h, H_2O_2 was added. ■, DOC; ●, MB; ▼, element C.

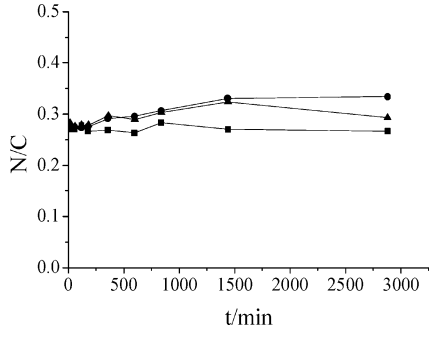

Figure 6. Changes of N/C value during the reactions of (■) no H_2O_2 added; (▲) MB and H_2O_2 added synchronously; and (●) H_2O_2 added after the addition of MB for 12 h.

after the treatment. So most of the MB removed from reaction solution by titanomagnetite (shown in Figure 2) was degraded.

Figure 6 presents the changes of N/C value on titanomagnetite during the reactions. It can be seen that the values of N/C for the degradation of MB are always higher than those for the adsorption of MB. So during the degradation of MB, compared with element C, element N was enriched on titanomagnetite. This indicates that the degradation products with N groups on their rings showed a higher degree of adsorption.[26,27]

Degradation Products. The mechanism of MB degradation by hydroxyl radical was proposed by Ma et al.[30] In the mechanism, the ultimate degradation product was mainly acetic acid, and aniline compounds may appear during the degradation. In our previous study, ^{13}C NMR findings indicate that the aromatic rings in MB were destroyed completely and the organic degradation products were mainly small molecule organic acids.[21] Chemical analysis results also indicate that the concentration of aniline compounds in reaction solution after the treatment was not detected. Because aniline compounds have $-NH_2$ on their rings, they may be easily adsorbed on titanomagnetite at neutral pH values.[26,27] Subsequently, the adsorbed aniline compounds would be degraded completely. This result is consistent with the analysis of N/C values on titanomagnetite.

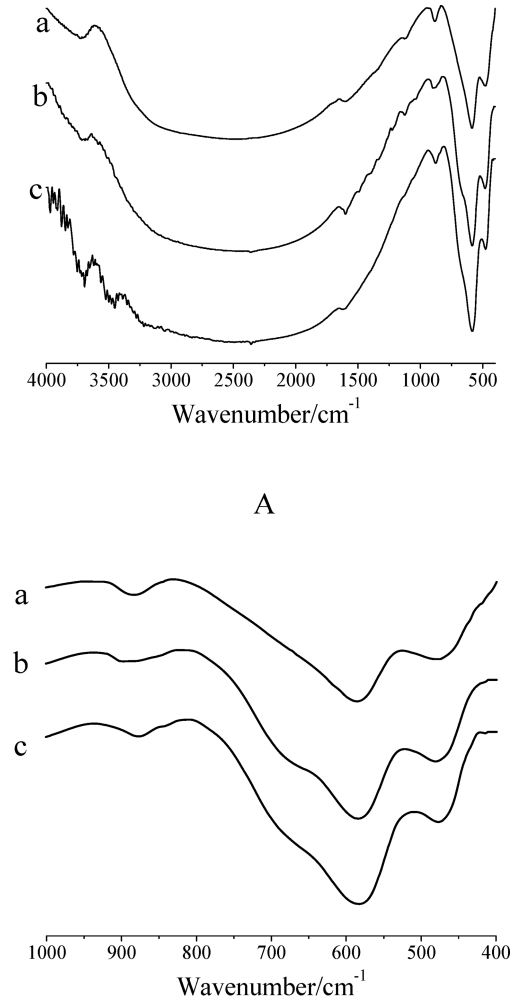

Figure 7. (A) FTIR spectra of (a) synthetic titanomagnetite; (b) synthetic titanomagnetite after the adsorption of MB on it for 24 h; and (c) synthetic titanomagnetite after the degradation of MB on it for 48 h. (B) Expansion of FTIR spectra from 400−1000 cm^{-1}.

FTIR Spectra Study. FTIR spectra for synthetic titanomagnetite and those after the degradation (48 h) and adsorption of MB on it were recorded (Figure 7A). As shown in Figure 7B-a,A-a, the infrared spectrum of synthetic titanomagnetite shows characteristic bands at about 470 cm^{-1}, 585 cm^{-1}, 890 cm^{-1}, and 3725 cm^{-1}. The band at about 585 cm^{-1} is the characteristic vibration of Fe−O in magnetite.[32,33] The vibration at about 470 cm^{-1} may be attributed to the Fe^{III}−O stretch vibration in maghemite structure.[34] The vibration at about 890 cm^{-1} is ascribed to the −OH bending mode.[35] It was suggested that a small amount of −OH in synthetic magnetite was a prerequisite for maghemite formation.[36] The vibration at about 3725 cm^{-1}

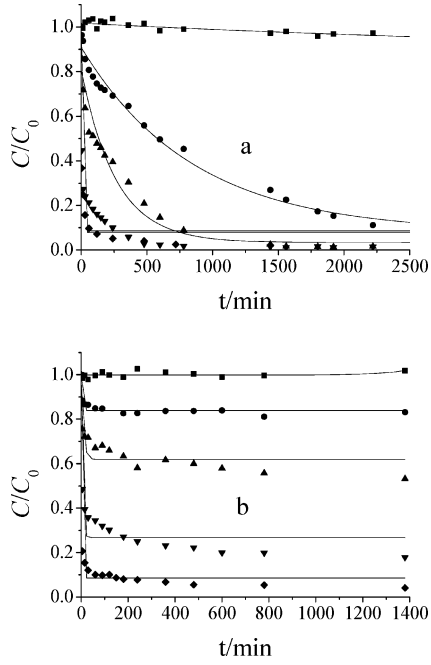

Figure 8. Influence of titanomagnetite load on the removal of MB: (a) MB and H_2O_2 were added synchronously; (b) no H_2O_2 was added. ■, titanomagnetite load = 0; ●, 0.5 g L^{-1}; ▲, 1.0 g L^{-1}; ▼, 2.0 g L^{-1}; ◆, 3.0 g L^{-1}.

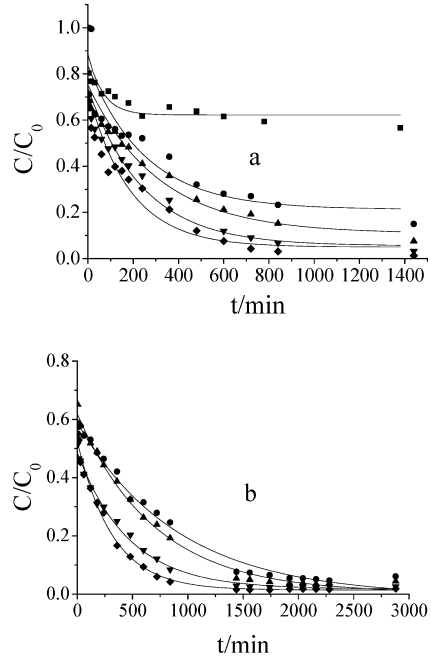

Figure 9. Influence of H_2O_2 concentration on the removal of MB: (a) MB and H_2O_2 were added synchronously; (b) after the addition of MB for 12 h, H_2O_2 was added. ■, H_2O_2 concentration = 0; ●, 0.075 mol L^{-1}; ▲, 0.15 mol L^{-1}; ▼, 0.30 mol L^{-1}; ◆, 0.45 mol L^{-1}.

is ascribed to the surface hydroxyl groups, which result from the hydration of titanomagnetite.[37]

As shown in Figure 7B-b,c, these characteristic vibrations of synthetic titanomagnetite all appear, and no other vibrations appear at 400−1000 cm^{-1}. This indicates that little phase change happened in titanomagnetite after the reactions. Moreover, the vibration at about 1050 cm^{-1} corresponding to phosphate does not appear. This indicates that no phosphate adsorbed on titanomagnetite at pH 6.8. So the interference of phosphatic buffer solution in the degradation and adsorption of MB on titanomagnetite can be neglected.

Compared with Figure 7A-a, Figure 7A-b shows some subtle vibrations at 1000−1500 cm^{-1}. The vibrations that appeared are ascribed to MB adsorbed on titanomagnetite. But these vibrations disappear in Figure 7A-c. This indicates that the adsorbed MB was degraded by titanomagnetite in the presence of H_2O_2. Furthermore, there are some vibrations that appeared at 3400−4000 cm^{-1} in Figure 7A-c. These vibrations are ascribed to the small molecule organic acids adsorbed on titanomagnetite, which result from the degradation of MB.

When there was little organics adsorbed on titanomagnetite, titanomagnetite would soon be oxidized by H_2O_2 and the color of titanomagnetite would turn from black to yellow. The oxidized particles were very difficult to separate from the reaction solution using centrifugation, filtering, or magnet.

3.3. Important Factors Affecting the Degradation of MB on Titanomagnetite. Influence of Titanomagnetite Load. For homogeneous Fenton processes, there is a direct correlation of organic contaminants removal efficiency with iron ion concentration, up to a certain concentration, where further addition of iron becomes inefficient.[38] The removal of MB by titanomagnetite (0−3.0 g L^{-1}) in the presence of H_2O_2 is displayed in Figure 8a. It shows that the removal of MB was promoted remarkably with the increase of titanomagnetite load. It indicates that no external mass transfer limitation occurred under this experimental condition. Other metal oxide catalysts showed similar results.[39] The enhancement due to catalyst addition was proposed to the promotion of H_2O_2 decomposition.[39] Furthermore, the adsorption of MB on titanomagnetite (0−3.0 g L^{-1}) was conducted (shown in Figure 8b). It shows that MB adsorbed on titanomagnetite was also increased remarkably with the increase of titanomagnetite load, which may be another important reason for the enhancement of MB removal.

Influence of H_2O_2 Concentration. Figure 9a depicts the effect of H_2O_2 concentration (0−0.45 mol L^{-1}) on the removal of MB by titanomagnetite. It shows that the residual MB in reaction solution decreased with the increase of H_2O_2 concentration. But the adsorption of MB on titanomagnetite was involved in the process of MB removal. To quantify the influence of H_2O_2 concentration on the degradation of MB, another experiment was conducted. In the experiment, H_2O_2 was added after the addition of MB for 12 h. As shown in Figure 9b, the further removal of MB after the addition of H_2O_2 (time zero) should be mainly attributed to the degradation of MB. The values of pseudo-first-order kinetic constants k for the degradation of MB (Figure 9b) are displayed in Table 1. It shows that the degradation of MB was promoted with the increase of H_2O_2 concentration. There is an excellent linear correlation between the pseudo-first-order kinetic constant k and H_2O_2 concentration ($R^2 = 0.992$). This result is consistent with the reports that H_2O_2 concentration was strongly proportional to the degradation of organics.[10,40]

Influence of Reaction Temperature. As reported in previous literatures, reaction temperature affected the degradation of organic contaminants.[38,40] This factor was also studied for titanomagnetite. Figure 10 presents the effect of reaction temperature (35−70 °C) on the degradation of MB. In this experiment, H_2O_2 was added after the addition of MB for 12 h. The values of pseudo-first-order kinetic constants k for the degradation of MB (Figure 10) are displayed in Table 1. It shows that the degradation of MB on titanomagnetite was promoted remarkably with the increase of reaction temperature. The temporal evolutions of UV−vis spectra taking place during the degradation of MB on titanomagnetite at different reaction

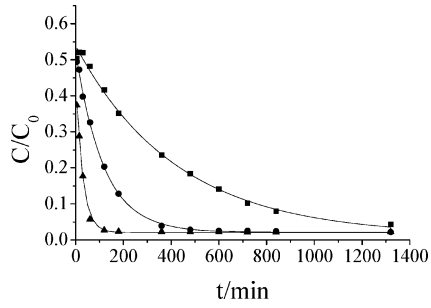

Figure 10. Influence of reaction temperature on the degradation of MB: ■, 35 °C; ●, 50 °C; ▲, 70 °C.

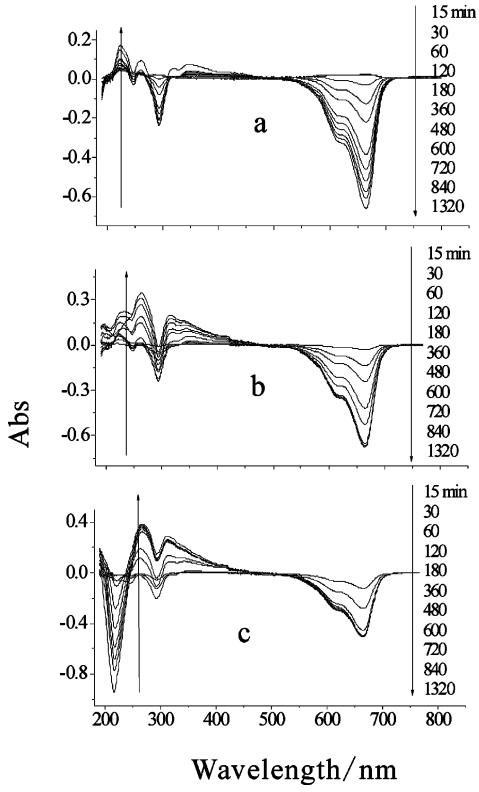

Figure 11. Changes of UV−vis spectra (after transformation) during the degradation of MB on titanomagnetite at (a) 35 °C; (b) 50 °C; (c) 70 °C.

temperatures (Figure 10) are displayed in Figure 11, in which the lines corresponding to 5 min were subtracted from all the lines as baselines. As shown in Figure 11, the negative peak at about 200 nm corresponding to the decomposition of H_2O_2 enhances remarkably with the increase of reaction temperature. This indicates that the decomposition of H_2O_2 was promoted remarkably with the increase of reaction temperature. It is well-known that a self-decomposition of H_2O_2 can occur at higher temperature. The blank experiment (MB + H_2O_2 with heating) was conducted. No MB was removed after this operation. It indicates that no hydroxyl radical formed during the self-decomposition of H_2O_2 and the degradation of MB (Figure 10) may be mainly attributed to free radical resulted from catalytic decomposition of H_2O_2 by titanomagnetite. So the enhancement of MB degradation due to the increase of reaction temperature corresponded to promoting the catalytic decomposition of H_2O_2 by titanomagnetite.

3.4. Stability Test. Stability is always an important issue for a catalyst to be applied in a plant-scale process from both catalytic and economic perspectives.[41] By repeating the degradation of MB for a number of runs, the lifespan of titanomagnetite can be estimated. As shown in Figure 5b, it took more than 48 h to degrade 100 mg L^{-1} of MB completely. To improve the operational efficiency, the run cycle was set as 24 h for the stability test. Figure 12 illustrates the catalytic efficiency of titanomagnetite during five repeated runs. It clearly shows that most MB can be removed for each run at 24 h reaction time.

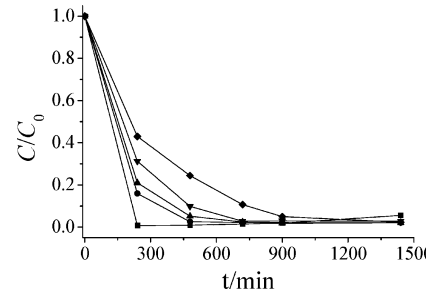

Figure 12. Stability test on the performance of titanomagnetite for the removal of MB: ■, 1st run; ●, 2nd run; ▲, 3rd run; ▼, 4th run; ◆, 5th run.

As shown in Figure 5b, there was some MB or organic intermediates adsorbed on titanomagnetite at 24 h reaction time in the first run. The organics adsorbed on titanomagnetite at the end of the first run would be introduced to the second run. The contents of element C on titanomagnetite after the first, second, third, fourth, and fifth runs were 0.39%, 1.42%, 1.51%, 1.56%, and 1.72%, respectively. This indicates that the actual load of organic pollutants for each run increased during the reusing. As a result, the removal efficiency of MB in the first 12 h for each run decreased (shown in Figure 12).

4. Conclusions

Titanomagnetite showed an excellent catalytic activity for the degradation of MB at neutral pH values. Although a small amount of MB was mineralized, the aromatic rings in MB were destroyed completely. This performance is a significant breakthrough to the conventional heterogeneous Fenton catalysts which have poor catalytic activity at neutral pH values without UV light for photolysis and are difficult to separate after the treatment.

Acknowledgment

This work was financially supported by National Natural Science Foundation of China (Grant 40773060) and "863" Exploration Program, the Ministry of Science and Technology of the People's Republic of China (Grant 2006AA03Z337). This is contribution No. IS-1112 from GIGCAS.

Nomenclature

MB = methylene blue
FTIR = Fourier transform infrared spectroscopy
DOC = dissolved organic carbon
SEM = scanning electronic microscopy

Supporting Information Available: Characterization of synthetic titanomagnetite using X-ray diffraction and Mössbauer spectroscopy. This material is available free of charge via the Internet at http://pubs.acs.org.

Literature Cited

(1) De Laat, J.; Gallard, H. Catalytic decomposition of hydrogen peroxide by Fe(III) in homogeneous aqueous solution: Mechanism and kinetic modeling. *Environ. Sci. Technol.* **1999**, *33*, 2726.

(2) Kwan, W. P.; Voelker, B. M. Decomposition of hydrogen peroxide and organic compounds in the presence of dissolved iron and ferrihydrite. *Environ. Sci. Technol.* **2002**, *36*, 1467.

(3) Kwan, W. P.; Voelker, B. M. Rates of hydroxyl radical generation and organic compound oxidation in mineral-catalyzed Fenton-like systems. *Environ. Sci. Technol.* **2003**, *37*, 1150.

(4) Kuo, W. G. Decolorizing dye waste-water with Fenton reagent. *Water Res.* **1992**, *26*, 881.

(5) Zepp, R. G.; Faust, B. C.; Hoigne, J. Hydroxyl radical formation in aqueous reactions (pH 3−8) of iron (II) with hydrogen peroxide: the photo-Fenton reaction. *Environ. Sci. Technol.* **1992**, *26*, 313.

(6) Lee, S.; Oh, J.; Park, Y. Degradation of phenol with Fenton-like treatment by using heterogeneous catalyst (modified iron oxide) and hydrogen peroxide. *J. Korean Chem. Soc.* **2006**, *27*, 489.

(7) Zazo, J. A.; Casas, J. A.; Mohedano, A. F.; Gilarranz, M. A.; Rodriguez, J. J. Chemical pathway and kinetics of phenol oxidation by Fenton's reagent. *Environ. Sci. Technol.* **2005**, *39*, 9295.

(8) Kornmuller, A.; Karcher, S.; Jekel, M. Adsorption of reactive dyes to granulated iron hydroxide and its oxidative regeneration. *Water Sci. Technol.* **2002**, *46*, 43.

(9) Tang, W. Z.; Chen, R. Z. Decolorization kinetics and mechanisms of commercial dyes by H_2O_2/iron powder system. *Chemosphere* **1996**, *32*, 947.

(10) Chou, S. S.; Huang, C. P. Application of a supported iron oxyhydroxide catalyst in oxidation of benzoic acid by hydrogen peroxide. *Chemosphere* **1999**, *38*, 2719.

(11) Chou, S. S.; Huang, C. P.; Huang, Y. H. Heterogeneous and homogeneous catalytic oxidation by supported γ-FeOOH in a fluidized bed reactor: Kinetic approach. *Environ. Sci. Technol.* **2001**, *35*, 1247.

(12) Gemeay, A. H.; Mansour, I. A.; El-Sharkawy, R. G.; Zaki, A. B. Kinetics and mechanism of the heterogeneous catalyzed oxidative degradation of indigo carmine. *J. Mol. Catal. A: Chem.* **2003**, *193*, 109.

(13) Kong, S. H.; Watts, R. J.; Choi, J. H. Treatment of petroleum-contaminated soils using iron mineral catalyzed hydrogen peroxide. *Chemosphere* **1998**, *37*, 1473.

(14) Tyre, B. W.; Watts, R. J.; Miller, G. C. Treatment of 4 biorefractory contaminants in soils using catalyzed hydrogen-peroxide. *J. Environ. Qual.* **1991**, *20*, 832.

(15) Costa, R. C. C.; de Fatima, M.; Lelis, F.; Oliveira, L. C. A.; Fabris, J. D.; Ardisson, J. D.; Rios, R.; Silva, C. N.; Lago, R. M. Remarkable effect of Co and Mn on the activity of $Fe_{3-x}M_xO_4$ promoted oxidation of organic contaminants in aqueous medium with H_2O_2. *Catal. Commun.* **2003**, *4*, 525.

(16) Costa, R. C. C.; Lelis, M. F. F.; Oliveira, L. C. A.; Fabris, J. D.; Ardisson, J. D.; Rios, R.; Silva, C. N.; Lago, R. M. Novel active heterogeneous Fenton system based on $Fe_{3-x}M_xO_4$ (Fe, Co, Mn, Ni): The role of M^{2+} species on the reactivity towards H_2O_2 reactions. *J. Hazard. Mater.* **2006**, *129*, 171.

(17) Junior, I. L.; Millet, J. M. M.; Aouine, M.; do Carmo Rangel, M. The role of vanadium on the properties of iron based catalysts for the water gas shift reaction. *Appl. Catal., A* **2005**, *283*, 91.

(18) Menini, L.; da Silva, M. J.; Lelis, M. F. F.; Fabris, J. D.; Lago, R. M.; Gusevskaya, E. V. Novel solvent free liquid-phase oxidation of β-pinene over heterogeneous catalysts based on $Fe_{3-x}M_xO_4$ (M = Co and Mn). *Appl. Catal., A* **2004**, *269*, 117.

(19) Oliveira, L. C. A.; Fabris, J. D.; Rios, R.; Mussel, W. N.; Lago, R. M. $Fe_{3-x}Mn_xO_4$ catalysts: Phase transformations and carbon monoxide oxidation. *Appl. Catal., A* **2004**, *259*, 253.

(20) Magalhaes, F.; Pereira, M. C.; Botrel, S. E. C.; Fabris, J. D.; Macedo, W. A.; Mendonca, R.; Lago, R. M.; Oliveira, L. C. A. Cr-containing magnetites $Fe_{3-x}Cr_xO_4$: The role of Cr^{3+} and Fe^{2+} on the stability and reactivity towards H_2O_2 reactions. *Appl. Catal., A* **2007**, *332*, 115.

(21) Yang, S. J.; He, H. P.; Wu, D. Q.; Chen, D.; Liang, X. L.; Qin, Z. H.; Fan, M. D.; Zhu, J. X.; Yuan, P. Decolorization of methylene blue by heterogeneous Fenton reaction using $Fe_{3-x}Ti_xO_4$ ($0 \leq x \leq 0.78$) at neutral pH values. *Appl. Catal., B* **2009**, *89*, 527.

(22) Baldrian, P.; Merhautova, V.; Gabriel, J.; Nerud, F.; Stopka, P.; Hruby, M.; Benes, M. J. Decolorization of synthetic dyes by hydrogen peroxide with heterogeneous catalysis by mixed iron oxides. *Appl. Catal., B* **2006**, *66*, 258.

(23) Kakol, Z.; Sabol, J.; Honig, J. M. Cation distribution and magnetic-properties of titanomagnetites $Fe_{3-x}Ti_xO_4$ ($0<x<1$). *Phys. Rev. B* **1991**, *43*, 649.

(24) Lin, S. S.; Gurol, M. D. Catalytic decomposition of hydrogen peroxide on iron oxide: Kinetics, mechanism, and implications. *Environ. Sci. Technol.* **1998**, *32*, 1417.

(25) Andreozzi, R.; Caprio, V.; Marotta, R. Oxidation of 3,4-dihydroxybenzoic acid by means of hydrogen peroxide in aqueous goethite slurry. *Water Res.* **2002**, *36*, 2761.

(26) Andreozzi, R.; D'Apuzzo, A.; Marotta, R. Oxidation of aromatic substrates in water/goethite slurry by means of hydrogen peroxide. *Water Res.* **2002**, *36*, 4691.

(27) He, J.; Ma, W. H.; Song, W. J.; Zhao, J. C.; Qian, X. H.; Zhang, S. B.; Yu, J. C. Photoreaction of aromatic compounds at α-FeOOH/H_2O interface in the presence of H_2O_2: Evidence for organic-goethite surface complex formation. *Water Res.* **2005**, *39*, 119.

(28) Satoh, A. Y.; Trosko, J. E.; Masten, S. J. Methylene blue dye test for rapid qualitative detection of hydroxyl radicals formed in a Fenton's reaction aqueous solution. *Environ. Sci. Technol.* **2007**, *41*, 2881.

(29) Houas, A.; Lachheb, H.; Ksibi, M.; Elaloui, E.; Guillard, C.; Herrmann, J. M. Photocatalytic degradation pathway of methylene blue in water. *Appl. Catal., B* **2001**, *31*, 145.

(30) Ma, H.; Zhuo, Q.; Wang, B. Characteristics of CuO-MoO_3-P_2O_5 catalyst and its catalytic wet oxidation (CWO) of dye wastewater under extremely mild conditions. *Environ. Sci. Technol.* **2007**, *41*, 7491.

(31) Patey, M. D.; Rijkenberg, M. J. A.; Statham, P. J.; Stinchcombe, M. C.; Achterberg, E. P.; Mowlem, M. Determination of nitrate and phosphate in seawater at nanomolar concentrations. *TrAC, Trends Anal. Chem.* **2008**, *27*, 169.

(32) Keiser, J. T.; Brown, C. W.; Heidersbach, R. H. The electrochemical reduction of rust film on weathering surfaces. *J. Electrochem. Soc.* **1982**, *129*, 2686.

(33) Poling, G. W. Infrared reflection studies of the oxidation of copper and iron. *J. Electrochem. Soc.* **1969**, *116*, 958.

(34) Cornell, R. M.; Schwertmann, U. *The iron oxides: Structure, properties, reactions, occurrences and uses*; Wiley-VCH: New York, 2003.

(35) Okamoto, S. Structure of δ-FeOOH. *J. Am. Ceram. Soc.* **1968**, *51*, 594.

(36) Sidhu, P. S.; Gilkes, R. J.; Posner, A. M. Oxidation and ejection of nickel and zinc from natural and synthetic magnetites. *Soil Sci. Soc. Am. J.* **1981**, *45*, 641.

(37) Busca, G.; Lorenzelli, V.; Ramis, G.; Willey, R. S. Surface sites on spinel type of corundum type mental oxide powders. *Langmuir* **1993**, *9*, 92.

(38) Catrinescu, C.; Teodosiu, C.; Macoveanu, M.; Miehe-Brendle, J.; Le Dred, R. Catalytic wet peroxide oxidation of phenol over Fe-exchanged pillared beidellite. *Water Res.* **2003**, *37*, 1154.

(39) Yu, R. B.; Xiao, F. S.; Wang, D.; Sun, J. M.; Liu, Y.; Pang, G. S.; Feng, S. H.; Qiu, S. L.; Xu, R. R.; Fang, C. G. Catalytic performance in phenol hydroxylation by hydrogen peroxide over a catalyst of V-Zr-O complex. *Catal. Today* **1999**, *51*, 39.

(40) Liou, R. M.; Chen, S. H.; Hung, M. Y.; Hsu, C. S.; Lai, J. Y. Fe (III) supported on resin as effective catalyst for the heterogeneous oxidation of phenol in aqueous solution. *Chemosphere* **2005**, *59*, 117.

(41) Lam, F. L. Y.; Yip, A. C. K.; Hu, X. J. Copper/MCM-41 as a highly stable and pH-insensitive heterogeneous photo-Fenton-like catalytic material for the abatement of organic wastewater. *Ind. Eng. Chem. Res.* **2007**, *46*, 3328.

Received for review April 27, 2009
Revised manuscript received July 14, 2009
Accepted August 13, 2009

IE900666B